Dalton Transactions

Accepted Manuscript

ROYAL SOCIETY OF CHEMISTRY

www.rsc.org/dalton

Journal Name

ARTICLE

Anion Binding, Electrochemistry and Solvatochromism of β-Brominated Oxoporphyrinogens

Received 00th January 20xx,
Accepted 00th January 20xx

DOI: 10.1039/x0xx00000x

www.rsc.org/

Whitney A. Webre,[a] Jonathan P. Hill,[b,*] Yoshitaka Matsushita,[c] Paul A. Karr,[d] Katsuhiko Ariga[b] and Francis D'Souza[a,*]

Effects of macrocycle bromination on the structural, electrochemical and anion binding properties of 5,10,15,20-tetrakis(3,5-di-t-butyl-4-oxo-cyclohexa-2,5-dienylidene)porphyrinogen, OxP, are reported. Bromination of 5,10,15,20-tetrakis(3,5-di-t-butyl-4-hydroxyphenyl)-porphinatocopper(II), [T(DtBHP)P]Cu(II) yielded β-Br_8OxP, which was N-alkylated to β-Br_8OxPBz_2 and β-Br_8OxPBz_4 (where Bz = 4-bromobenzyl). β-Br_8OxPBz_2 crystallizes in orthorhombic space group Pccn [a = 23.5535(17) Å, b = 19.3587(14) Å c = 20.9760(15) Å, V = 9564.3(12) $Å^3$]. It has a calix[4]pyrrole-like structure with a saddle conformation and two molecules of methanol occupy a central binding site made up of the non-alkylated pyrrole N-H groups. Computational and electrochemical studies revealed widening HOMO-LUMO band gaps for the brominated compounds over the non-brominated analogues consistent with the observed hypsochromic shifts in electronic absorption spectra. Solvatochromic and chromogenic effects on anion binding were both observed for β-Br_8OxP and β-Br_8OxPBz_2 with binding affinities of anions being greater than those observed for the corresponding OxP and OxPBz2. Colorimetric sensor studies suggest that the OxP compounds reported here are possible candidates for use in the design of optoelectronic noses for detection of anions and anionic analyte species of biological interest.

Introduction

Anion complexation using synthetic receptors is a burgeoning area of supramolecular chemistry[1] and has involved different classes of compounds including urea-based receptors,[2] calixarenes[3] and oligo-amide cryptands.[4] Also, sensing and transport of anions is an important area of investigation due to the presence of anions in many biological processes, making their analysis a matter of clinical application,[5] or because of the high toxicities of species such as fluoride and cyanide.[6] The relevant area of supramolecular chemistry involves preparation of molecular species that can operate as reporters,[7] usually through selective binding of the analyte anion, or as transport agents.[8] The latter may also find application as therapeutic agents for certain disease states which involve defects in metabolic processes.[9] Selective binding agents are also useful for anion separations either by liquid-liquid extraction or chromatographic means[10a-g] and modulating electron transfer properties in donor-acceptor supramolecular systems.[10h]

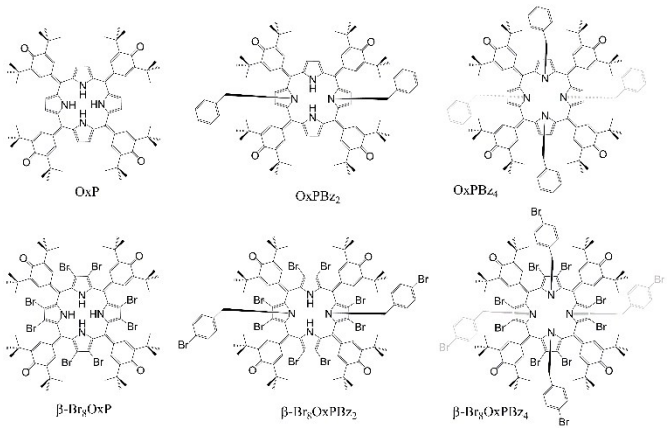

Figure 1. Structures of oxoporphyrinogens (unbrominated and brominated) and abbreviations used in the present study.

Calix[4]pyrroles[11] make up a class of compound that has been intensively studied for purposes of anion binding because of simple, high-yielding synthetic procedures including a wide range of modifications, which can be used to improve anion binding selectivity[12] or to introduce other functionalities.[13] For example, halogenation of calix[4]pyrrole improves their anion binding strengths while concurrently reducing their polarities making them suitable as anion sequestration reagents.[14] Bromination, in particular, has been applied in the synthesis of β-octabrominated calix[4]pyrroles.[15,16] The parent β-octabromocalix[4]pyrrole was found to have increased binding affinities for halides and dihydrogenphosphate suggesting its

[a] Department of Chemistry, University of North Texas, 1155 Union Circle, #305070, Denton, Texas 76203, USA. Tel: +940-369-8832; Fax: +940-565-4318; E-mail: Francis.Dsouza@unt.edu
[b] WPI Center for Materials Nanoarchitectonics, National Institute for Materials Science, Namiki 1-1, Tsukuba, Ibaraki 305-0044, Japan. Tel: +81298604399; Fax: +81298604832; E-mail: Jonathan.Hill@nims.go.jp
[c] Research Network and Facility Services Division, National Institute for Materials Science (NIMS), 1-2-1 Sengen, Tsukuba, Ibaraki 305-0047, Japan.
[d] Department of Physical Sciences and Mathematics, Wayne State College, 111 Main Street, Wayne, Nebraska, 68787, USA.
† Footnotes relating to the title and/or authors should appear here.
Electronic Supplementary Information (ESI) available: [details of any supplementary information available should be included here]. See DOI: 10.1039/x0xx00000x

use for removal of phosphate-based contaminants from aqueous environments.[14]

In previous work, we have studied the anion binding and solvatochromic properties of the calix[4]pyrrole analogue 5,10,15,20-tetrakis(3,5-di-t-butyl-4-oxo-cyclohexa-2,5-dienyl idene)-porphyrinogen, OxP.[17,18] OxP is a two-electron oxidized form of *meso*-tetrakis(3,5-di-t-butyl-4-hydroxyphenyl)-porphyrin,[18] which contains hemiquinone substituents at its *meso*-positions rather than the simple alkyl or aryl substituents contained in typical calix[4]pyrroles (see Figure 1 for structures). These substituents make up a delocalized electronic system conjugated with the tetrapyrrole macrocycle endowing OxP with a substantial optical absorption in the visible region. This in turn permits study of OxP for its colorimetric response to solvents (solvatochromism) or anions interacting with the macrocycle through hydrogen bonding with its pyrrolic N-H protons.[17] An additional feature of the OxP macrocycle is that it may be selectively N-alkylated at N_{21} and N_{23} leading to a highly conjugated calix[4]pyrrole core with a single binding site composed of unalkylated pyrrole groups of N_{22} and N_{24} (Figure 1),[19,20] which facilitates the study of guest binding and dynamics.[21] Since bromination of calix[4]pyrroles causes variation in the guest binding strengths,[14,16] we supposed that the same process applied to OxP could also lead to variation of its properties in interactions with guests and that there should also be a significant variation in the electronic absorptive properties of brominated OxP derivatives over the parent OxP. In this work, we present the synthesis and related properties of β-octabrominated-OxP and its bis-N-alkylated derivative (see Figure 1 for structures) with a view to assessing the potential of this class of compounds for anion sensing and other applications.

EXPERIMENTAL

Materials

The OxP derivatives used in this study were prepared by previously reported methods.[19] Dehydrated solvents (in septum-sealed bottles) used for spectroscopic measurements were obtained from Wako Chemical Co. or Aldrich Chemical Co reagents and were used without further purification. Tetra-n-butylammonium salts for anion binding studies were obtained from Aldrich Chemical Co., Tokyo Kasei Chemical Co. and Wako Chemical Co. Preparative thin layer chromatography plates were obtained from Analtech, 75 Blue Hen Drive, Newark, DE.

Electronic absorption spectra were measured using JASCO V-570 UV/Vis/NIR spectrophotometer, Princeton Applied Research (PAR) diode array rapid scanning spectrometer or a Shimadzu UV/Visible spectrophotometer. FTIR spectra were obtained from samples deposited on a barium fluoride disc using a Thermo-Nicolet 760X FTIR spectrophotometer. ^{1}H-NMR spectra were obtained using JEOL AL300BX or Bruker AM400 spectrometers using tetramethylsilane as an internal standard. MALDI-TOF mass spectra were measured using a Shimadzu Axima AFR+ mass spectrometer with dithranol as matrix. Computational geometry optimizations were performed at the B3LYP/3-21G level using NWChem.[22] The GaussView program of GAUSSIAN was used to generate frontier HOMO and LUMO orbitals. Cyclic voltammograms were recorded on an EG&G Model 263A potentiostat using a three electrode system. A platinum button electrode was used as the working electrode. A platinum wire served as the counter electrode and an Ag/AgCl electrode was used as the reference. Ferrocene/ferrocenium redox couple was used as an internal standard. All the solutions were purged prior to electrochemical and spectral measurements using argon gas. Spectroelectrochemical study was performed by using a cell assembly (SEC-C) supplied by ALS Co., Ltd. (Tokyo, Japan). This assembly comprised of a Pt counter electrode, a 6 mm Pt Gauze working electrode, and an Ag/AgCl reference electrode in a 1.0 mm path length quartz cell. The optical transmission was limited to 6 mm covering the Pt gauze working electrode.

Spectroscopic studies of anion binding were performed in dry non-deaerated *o*-dichlorobenzene (DCB) with a range of added tetrabutylammonium salts. For solvatochromism studies, the OxP derivatives (~10^{-4} M) were similarly dissolved in pure dry solvents without exclusion of air.

Synthesis

2,3,7,8,12,13,17,18-Octabromo-5,10,15,20-tetrakis(3,5-di-*t*-butyl-4-oxo-cyclohexa-2,5-dienylidene)porphyrinogen, β-**Br$_8$OxP**. 5,10,15,20-Tetrakis(3,5-di-t-butyl-4-hydroxyphenyl)porphinatocopper(II), [T(DtBHP)P]Cu(II), was brominated according to the method of Bhyrappa and Krishnan[23] except that pyridine was not added to the reaction mixture. [T(DtBHP)P]Cu(II) (300 mg, 2.5 × 10^{-4} mol) was dissolved in chloroform (100 mL) then bromine (0.5 mL) in chloroform (10 mL) was added dropwise over a period of 20 mins. The mixture was stirred and the progress was monitored using thin layer chromatography (SiO_2, $CHCl_3$) until no starting material remained (~3 h), then stirred for a further 2 h. The reaction mixture was poured into water then washed with aqueous sodium thiosulfate. The organic fraction was collected, dried (anhyd. Na_2SO_4) then solvents were removed under reduced pressure. The resulting residue was subject to flash chromatography (SiO_2, $CHCl_3$). Product containing fractions were collected. The main product was the 2-electron oxidized and demetallated oxporphyrinogen derivative 2,3,7,8,12,13,17,18-octabromo-5,10,15,20-tetrakis(3,5-di-*t*-butyl-4-oxo-cyclohexa-2,5-dienylidene)porphyrinogen, β-Br_8OxP. Further purification was achieved by layering a solution of Br_8OxP in $CHCl_3$ with the same volume of CH_2Cl_2 and refrigerating at −20 °C. Dark olive green amorphous powder. Yield: 64 %. ^{1}H NMR (300 MHz, 313 K, $CDCl_3$): δ = 1.29 (s, 72H, *t*Bu-H), 6.95 (s, 8H, cyclohexadienylidene-H), 9.04 (s, 4H, NH) ppm. ^{13}C NMR (75 MHz, 313 K, $CDCl_3$): δ = 29.5, 35.6, 109.1 (br.), 123.4 (br.), 130.8, 130.9, 133.4 (br.), 149.5, 186.4 ppm. FTIR (BaF_2): *v* = 3666.9 (w), 3600.4 (w), 3083.1 (w), 2997.3 (w), 2956.8 (s), 2921.9 (s), 2853.9 (m), 1586.9 (s), 1558.9 (m), 1505 (s), 1488.9 (m), 1459.1 (s), 1452.3 (s), 1399.4 (w), 1386.0 (m), 1375.6 (w), 1358.6 (s), 1330.9 (s), 1286.6 (s), 1263.3 (s), 1253.8 (s), 1200.2 (m), 1181.6 (w), 1115.7 (w), 1086.2 (s), 1048.3 (w), 1018.1 (s), 963.9 (s), 929.1 (w), 906.2 (m), 887.0 (w), 865.1 (s) cm^{-1}. MALDI-TOF-MS (dithranol): calculated for $[C_{76}H_{84}Br_8N_4O_4]^+$ = 1755.99; found: $[C_{76}H_{84}Br_8N_4O_4]^+$ = 1756.18 ($[M]^+$).

N_{21},N_{22}-*Bis*(4-bromobenzyl)-2,3,7,8,12,13,17,18-octabromo-5,10,15,20-tetrakis(3,5-di-*t*-butyl-4-oxo-cyclohexa-2,5-dienylidene)porphyrinogen (β-**Br$_8$OxPBz$_2$**) and **N_{21},N_{22},N_{23},N_{24}-Tetrakis(4-bromobenzyl)-2,3,7,8,12,13,17,18-octabromo-5,10,15,20-tetrakis(3,5-di-*t*-butyl-4-oxo-cyclohexa-2,5-dienylidene)porphyrinogen,** (β-**Br$_8$OxPBz$_4$**). A crude sample of β-**Br$_8$OxP** (300 mg, 1.71 × 10^{-4} mol) was subjected to N-alkylation initially using 4-bromobenzyl bromide (70 mg, 2.81 × 10^{-4} mol) in refluxing tetrahydrofuran (15 mL) in the presence of excess potassium carbonate according to a literature procedure.[19] A further aliquot of 4-bromobenzyl bromide (50 mg, 2.00 × 10^{-4} mol) was added after ~ 2 h. The reaction was monitored throughout using thin layer chromatography (SiO_2, CH_2Cl_2) until most of the starting β-Br_8OxP had been consumed. The reaction mixture was then cooled to room temperature, poured into water (50 mL) and extracted using chloroform (100 mL × 3). A persistent red solid precipitate in the water phase was also collected by filtration. Fractions from the extraction were combined, dried (anhyd. Na_2SO_4) and solvents removed under reduced pressure. The resulting orange solid residue was subjected first to flash chromatography (SiO_2, CH_2Cl_2) for collection of the two crude main products then (following evaporation of the solvents) each crude product

was subjected to preparative thin layer chromatography on SiO_2 plates eluting with CH_2Cl_2:n-hexane 70:30 v/v. Two main products were isolated:

β-Br_8OxPBz$_2$: red amorphous powder, yield: 41 % based on crude β-Br_8OxP. ^{1}H NMR (300 MHz, 298 K, $CDCl_3$): δ = 1.18 (s, 36H, *t*Bu-H), 1.33 (s, 36H, *t*Bu-H), 4.41 (s, 4H, benzylic-CH_2), 6.57 (d, 4H, cyclohexadienylidene-H, ^4J = 2.1 Hz), 7.07 (d, 4H, cyclohexadienylidene-H, ^4J = 2.1 Hz), 7.1 (overlapped, 4H, 4-BrBz-ArH), 7.31 (d, 8H, 4-BrBz-ArH, ^3J = 8.1 Hz), 9.14 (s, 2H, pyrrole NH) ppm. ^{13}C NMR (75 MHz, 303 K, $CDCl_3$): δ = 29.4, 29.45, 35.4, 35.7, 50.1, 108.8, 109.8, 123.0, 123.1, 130.1, 130.6, 131.2, 132.1, 132.8, 134.4, 134.9, 149.7, 149.8, 186.2 ppm. FTIR (BaF_2): *v* = 3633.7 (w), 3592.3 (w), 3074.1 (w), 3000.3 (w), 2958.1 (s), 2920.9 (m), 2867.4 (m), 1641.3 (w), 1610.9 (s), 1559.3 (w), 1540.6 (w), 1505.9 (w), 1487.7 (m), 1454.3 (m), 1407.4 (w), 1384.4 (m), 1361.5 (s), 1333.2 (m), 1308.7 (m), 1255.6 (m), 1198.7 (w), 1179.8 (w), 1121.1 (w), 1086.9 (m), 1074.3 (m), 1021.5 (m), 1014.6 (w), 962.0 (m), 929.8 (w), 910.7 (w), 894.9 (w), 879.3 (w) cm^{-1}. MALDI-TOF-MS (dithranol): calculated for $[C_{90}H_{94}Br_{10}N_4O_4]^+$ = 2093.91; found: $[C_{90}H_{94}Br_{10}N_4O_4]^+$ = 2093.98 ($[M]^+$).

β-Br_8OxPBz$_4$[24]: orange amorphous powder, yield: ~ 5 % based on crude β-Br_8OxP. ^{1}H NMR (300 MHz, 313 K, $CDCl_3$): δ = 1.23 (s, 72H, *t*Bu-H), 4.49 (s, 8H, benzylic-CH_2), 6.83 (d, 8H, 4-BrBz-ArH, ^3J = 8.4 Hz), 6.86 (s, 8H, cyclohexadienylidene-H), 7.25 (obscured by $CHCl_3$, β-pyrrole-H), 7.31 (d, 8H, 4-BrBz-ArH, ^3J = 8.4 Hz) ppm. ^{13}C NMR (75 MHz, 313 K, $CDCl_3$): δ = 29.4, 35.6, 48.9, 110.5, 122.1, 122.3, 128.2, 130.1, 131.9, 134.1, 135.4, 136.9, 150.3, 185.9 ppm. FTIR (BaF_2): *v* = 2999.7 (w), 2956.9 (s), 2922.4 (s), 2866.9 (m), 1642.5 (m), 1620.6 (m), 1611.4 (s), 1574.9 (w), 1560.4 (w), 1540.6 (w), 1513.9 (w), 1505.8 (w), 1490.2 (m), 1453.6 (m), 1420.0 (w), 1406.9 (w), 1371.9 (m), 1361.2 (m), 1332.8 (m), 1318.9 (m), 1255.1 (m), 1200.2 (w), 1170.3 (w), 1089.5 (w), 1072.3 (m), 1022.2 (m), 1012.8 (m), 976.4 (w), 959.5 (m), 928.5 (w), 910.8 (m) cm^{-1}. MALDI-TOF-MS (dithranol): calculated for $[C_{104}H_{106}Br_{12}N_4O_4]^+$ = 2433.84; found: $[C_{104}H_{105}Br_{12}N_4O_4]^+$ = 2433.71 ($[M + 2H]^+$).

X-ray Crystallography.‡ Crystals of β-Br_8OxPBz$_2$ were grown by diffusion of methanol into solutions of the compounds in chloroform. Data collections were performed using MoKα radiation (λ = 0.71073 Å) on a RIGAKU VariMax Saturn diffractometer equipped with a CCD detector. Prior to the diffraction experiment the crystals were flash-cooled to 110 K in a stream of cold N_2 gas. Cell refinements and data reductions were carried out by using the d*trek program package in the CrystalClear software suite.[25] The structures were solved using a dual-space algorithm method (SHELXT)[26] and refined by full-matrix least squares on F^2 using SHELXL-2014[27] in the WinGX program package.[28] Non-hydrogen atoms were anisotropically refined and hydrogen atoms were placed on calculated positions with temperature factors fixed at 1.2 times Ueq of the parent atoms and 1.5 times Ueq for methyl groups. Crystal data for β-Br_8OxPBz$_2$: green cuboid, $C_{180}H_{188}Br_{20}N_8O_{11}$, M_r = 4237.57, orthorhombic *P*ccn (56), a = 23.5535(17) Å, b = 19.3587(14) Å c = 20.9760(15) Å, V = 9564.3(12) Å^3, T = 113 K, Z = 2, R_{int} = 0.0611, GoF = 1.056, R_1 = 0.0726, wR(all data) = 0.2368.

RESULTS AND DISCUSSION

Synthesis.

Direct bromination of OxP using neat Br_2[29] or N-bromosuccinimide in tetrahydrofuran[30] failed with reactions leading to complex mixtures of products, and none of the required Br_8OxP product could be detected by mass spectrometric screening of those reactions. Treatment of OxP with bromine in chlorinated solvents[16] (chloroform, carbon tetrachloride or their mixtures) also gave only intractable mixtures. Attempts were also made to brominate the porphyrin precursor to OxP, 5,10,15,20-tetrakis(3,5-di-t-butyl-4-hydroxyphenyl)porphyrin (TDtBHPP). However, perhaps not surprisingly given its sensitivity to oxidation,[18,31] its treatment with neat bromine lead to further intractable products. Only when bromination was applied to the metal complexes of TDtBHPP was any progress made and finally a literature method[23] was identified as being the optimum route to β-Br_8OxP. Following our initial failure to β-brominate OxP, we had speculated that a three-step route would be required to obtain Br_8OxP. That is, (1) bromination of a metal complex of TDtBHPP (i.e. Cu^{2+}, Ni^{2+} Zn^{2+}) followed by (2) demetallation to the free base form, and (3) its oxidation under basic conditions. Surprisingly, when the method of Bhyrappa and Krishnan[23] was applied to 5,10,15,20-tetrakis(3,5-di-t-butyl-4-hydroxyphenyl)-porphinatocopper(II) the main product was β-Br_8OxP (~60% yield), and the anticipated subsequent steps of demetallation and oxidation were not required!

TDtBHPP is prone to oxidation under aerobic conditions in the presence of acid or base.[18,31,32] This is due either to increased mesomeric interaction between phenolate substituents (in the case of base) and the porphyrin macrocycle, which increases electron density on the macrocycle facilitating oxidation by O_2, or due to distortion of the macrocycle (in the case of acid) caused by protonation at the macrocycle nitrogen atoms. Thus, metal complexes of TDtBHPP generally resist oxidation since the porphyrin macrocycle is rigid[33] and cannot undergo structural changes implied by changes in oxidation state.[34] β-bromination apparently promotes oxidation to such an extent that oxidation/demetallation to the β-Br_8OxP product occurs. This is likely to be as a result of the increased distortion of the macrocycle caused by β-bromination since this would allow a higher degree of interaction with its electron rich phenolic substituents leading to a greater susceptibility to the 2-electron oxidation of the macrocycle. Thus, β-Br_8OxP is formed as the main product and was isolated easily in a crude but useful form by simple precipitation and filtration. The exact point at which demetallation/oxidation of the copper(II) complex occurs is unclear and it has also not been determined whether oxidation is preferred because of electronic or steric effects; these matters will be investigated later. Also, attempts to reduce β-Br_8OxP to its porphyrinic state suggest that the metal free β-Br_8TDtBHPP is quite unstable against oxidation with a rather rapid auto-oxidation in air back to the β-Br_8OxP form. Having finally obtained the required β-Br_8OxP molecule, we set about investigating its properties and the properties of its N-alkylated derivatives. For consistency with our recent work[35] and because of improvements in solubility gained by introducing bromine atoms at the benzylic 4-positions, we N-alkylated β-Br_8OxP using 4-bromobenzyl bromide giving N_{21},N_{23}-bis(4-bromobenzyl)-2,3,7,8,12,13,17,18-octabromo-5,10,15,20-tetrakis(3,5-di-t-butyl-4-oxo-cyclohexa-2,5-dienylidene)porphyrinogen (abbrv. β-Br_8OxPBz$_2$) and N_{21},N_{22},N_{23},N_{24}-tetrakis(4-bromobenzyl)-2,3,7,8,12,13,17,18-octabromo-5,10,15,20-tetra kis(3,5-di-t-butyl-4-oxo-cyclohexa-2,5-dienylidene)porphyrinogen (abbrv. β-Br_8OxPBz$_4$) as the main products. These were separated by column chromatography and crystallized by diffusion of methanol into their respective solutions in chloroform. For the purposes of this study, a sample of β-Br_8OxP was also purified by column

chromatography and recrystallized; although crystals suitable for X-ray crystallography could not be obtained in that case.

Structure

Crystals of β-Br_8OxPBz_2 and β-Br_8OxPBz_4[24] suitable for X-ray crystallography were obtained by diffusion of methanol into individual solutions in chloroform. The crystal structure of β-Br_8OxPBz_4 (Figure S1) has already been reported by us but is less important in this case since it does not strongly interact with solvents or anionic species under the conditions applied here. β-Br_8OxPBz_2 contains a site that can interact with polar inorganic species including anions. In fact, its structure (Figure 2) contains two molecules of cosolvent methanol hydrogen bonded at this site, which is composed of the two non-N-alkylated pyrrole groups.[19-21] Methanol molecules are strongly disordered in contrast with what is usually observed, which is probably due to some free rotation of the methanol guests about the single hydrogen bonds. In cases where a single guest is bound through two hydrogen bonds, good ordering of the guest is found.[17,19] A comparison of the X-ray crystal structure of β-Br_8OxPBz_2 with that of the non-brominated analogue OxPBz_2 is also shown in Figure 2.

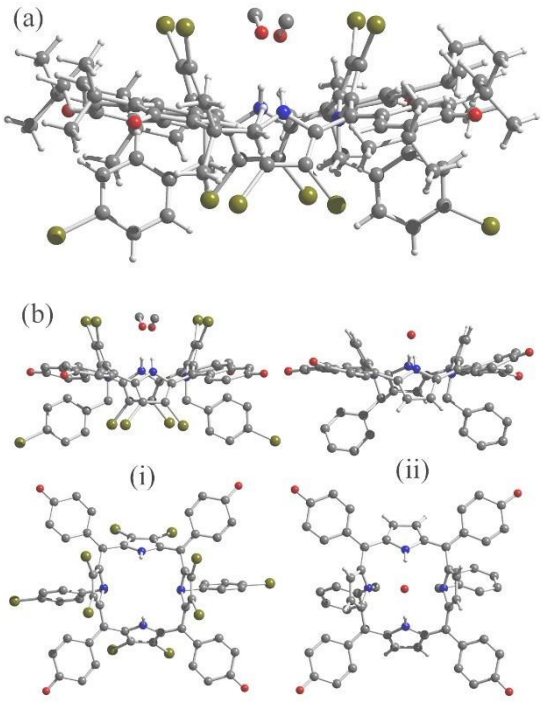

Figure 2. (a) X-ray structure of β-Br_8OxPBz_2. (b) Edge and plane views of (i) β-Br_8OxPBz_2 and (ii) OxPBz_2[19] for a comparison of their skeletal structures. Protons and *t*-butyl groups removed for clarity. In the plan view of β-Br_8OxPBz_2 the methanol guests have also been removed for clarity. Atom colours: C (grey), H (white), N (blue), O (red), Br (olive green).

The presence of bromine atoms at the pyrrolic β-positions has a significant effect on the conformation of the macrocycle causing a more substantial departure from planarity than observed for OxPBz_2. This is most conveniently described by considering the angles subtended between different planes within the molecules. These are shown in Table 1 for β-Br_8OxPBz_2 and OxPBz_2. OxPBz_2 is much more distorted (i.e. less symmetrical) than β-Br_8OxPBz_2 with respect to the angles between the pyrrole groups and its macrocyclic mean plane (defined by C and N atoms composing the macrocycle not including the pyrrole β-carbon atoms). Angles subtended by pyrrolic planes and the mean plane are 46.97° and 52.46° for non-alkylated pyrroles and 60.64° and 67.86° for N-alkylated pyrrole groups indicating the lower symmetry of OxPBz_2. Angles subtended by the *meso*-substituents are also variable for OxPBz_2 suggesting some conformational flexibility in this molecule. Crystallographic packing forces may also contribute to the distortion of OxPBz_2. Other notable parameters for OxPBz_2 are the angles subtended between opposing pyrrole planes, which are 51.51° and 80.58 for N-alkylated and N-H pyrrole groups, respectively. Bromination of the macrocyclic β-positions has the effect of forcing the OxP molecule into a more symmetrical conformation largely due to interactions between bromine atoms and *meso*-substituents. In fact, the crystallographic asymmetric unit contains half of the β-Br_8OxPBz_2 molecule. Angles subtended by *meso*-substituents and macrocyclic mean plane are quite similar at 13.61° and 15.67° while the difference in the angles between N-alkylated and N-H pyrrole groups and the macrocyclic plane (71.74° and 63.52°, resp.) is only 12° compared to up to ~ 21° for OxPBz_2. As expected based on the increased steric constraints in β-Br_8OxPBz_2, the angles subtended between opposing pyrrole groups at 36.51° (N-alkyl) and 52.95° (N-H) are more acute than for OxPBz_2 but are also more similar than for OxPBz_2 where there is a ~ 29° difference in this parameter. Bond lengths in the two molecules are comparable although there is slight (0.01 Å) shortening of the double bonds connecting the *meso*-substituents to the macrocycle. Although the intramolecular interaction between the β-bromine atoms in β-Br_8OxPBz_2 might be considered a steric force, there is also the possibility that this interaction is due to hydrogen bonding. This is highlighted by the close approach of the bromine atoms to the alkene protons of the *meso*-substituents, and the Br…H distances at around 3 Å are appropriate for an intramolecular H-bonding interaction.[36]

Table 1. Angles (°) subtended between macrocyclic planes in OxPBz_2 and β-Br_8OxPBz_2.

Subtended Angle	OxPBz_2		β-Br_8OxPBz_2	
Macrocycle[a]/ pyrrole planes	non-alkylated 46.97, 52.46	N-alkylated 60.64, 67.86	non-alkylated 63.52[b]	N-alkylated 71.74[b]
Macrocycle[a]/ *meso*-substituent	3.59, 7.19, 21.02, 11.77		15.67, 13.61	
Opposing pyrrole groups	non-alkylated 80.58	N-alkylated 51.51	non-alkylated 52.95	N-alkylated 36.51
Adjacent pyrroles	68.83, 76.29, 76.49, 73.34		79.07, 84.85	

[a]Macrocyclic mean plane defined by C and N atoms and excluding pyrrolic β-carbon atoms.

[b]High symmetry leads to single values.

Electronic Absorption Spectra

Figure 3 shows the optical absorption spectra of brominated OxPs (while the data is summarized in Table 2, which also lists data for unbrominated derivatives for comparative purposes (log ε at absorbance maximum is listed). In agreement with the earlier reported OxP derivatives, brominated OxPs (β-Br_8OxP, β-Br_8OxPBz_2 and β-Br_8OxPBz_4 revealed broad spectra with an absorption maximum in the 450-500 nm range. Another less intense peak in the 300-350 nm range can also be observed. For each OxP derivative, β-octabromination causes a blue shift in the range of 1,000-1,300 cm^{-1}. This observed blue shift for these brominated OxP derivatives is in contrast to that reported earlier for tetraphenylporphyrin (TPP) where the β-octabrominated porphyrin derivative (Br_8TPP) undergoes a red shift of its absorption maximum of about 2,500 cm^{-1}. In the case of TPP, there are two main factors contributing to the red shift: inductive effects caused by electron-withdrawing bromine

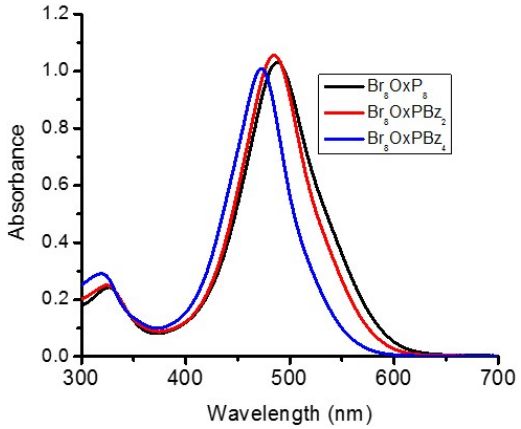

Figure 3. Electronic absorption spectra of β-Br_8OxP, β-Br_8OxPBz_2 and β-Br_8OxPBz_4 in *o*-dichlorobenzene.

Table 2. Electronic absorption data for OxP, OxPBz_2 and OxPBz_4 and their octabrominated analogues in neutral, oxidized and reduced forms in *o*-dichlorobenzene.

Compound	OxP, λ nm (log ε)	OxP^+, λ nm	OxP^-, λ nm
OxP[a]	375, 518 (4.82)	455, 698	475, 555, 785
β-Br_8OxP	344, 487 (5.11)	385, 613, 759	405, 550, 659
OxPBz_2	334, 509 (4.94)	525, 750	350, 572, 744
β-Br_8OxPBz_2	334, 485 (5.07)	498, 613(sh), 738	386, 546, 646
OxPBz_4	333, 504 (4.99)	418(sh), 502	505, 575(sh), 718
β-Br_8OxPBz_4	321, 472 (4.94)	468	475, 696, 811

[a]-irreversible spectral changes during oxidation and reduction
sh = shoulder band

substituents, and the significant non-planarity of the porphyrin ring caused by β-bromination. For OxP, however, its macrocycle is already substantially nonplanar so that β-bromination does not cause as significant relative deformation as for TPP as revealed by X-ray and computational (*vide supra*) studies. Thus, inductive effects caused by the introduction of bromo substituents should be the main contributors to the blue shift observed in case of brominated OxP although increased angles between pyrrole planes and *meso*-substituents must also contribute.

Computational Studies

In order to gain insight into the geometry of the brominated OxP derivatives, computational studies were performed using density functional methods (DFT) at the B3LYP/3-21G level. In these calculations, all of the compounds, built from scratch using *GaussView*, were fully optimized to a stationary point on the Born-Oppenheimer potential energy surface. The space filling models of the computed structures are shown on the left-hand side of Figure 4. In order to assess the computed structures, especially with regard to the effect of β-pyrrole bromination on the relative non-planarity of the compounds, the computed structures were compared with the known X-ray structures of OxP, OxPBz_2 and OxPBz_4. The results of the comparison are depicted in the flat-scale projections shown on the right side of Figure 4. The flat-scale projections were generated by least squares fitting of a plane to the 24 C and N atoms of the porphyrin ring, establishing the origin of the plane at the centroid of the 24 atoms, defining the positive X-axis in the direction of one of the *meso*-carbons, the positive Y-axis orthogonal to X in the direction of another one of the *meso*-carbons, and the positive Z axis orthogonal to the XY plane. The original atomic coordinates were transformed to the newly defined coordinate system, and the Z coordinate plotted against the arctangent of the XY coordinates. For compound β-Br_8OxP bearing no N-substituents, skeletal deformations were close to those of unbrominated OxP. The β-pyrrole carbons were displaced as much as 1.7 Å from the least squares plane.

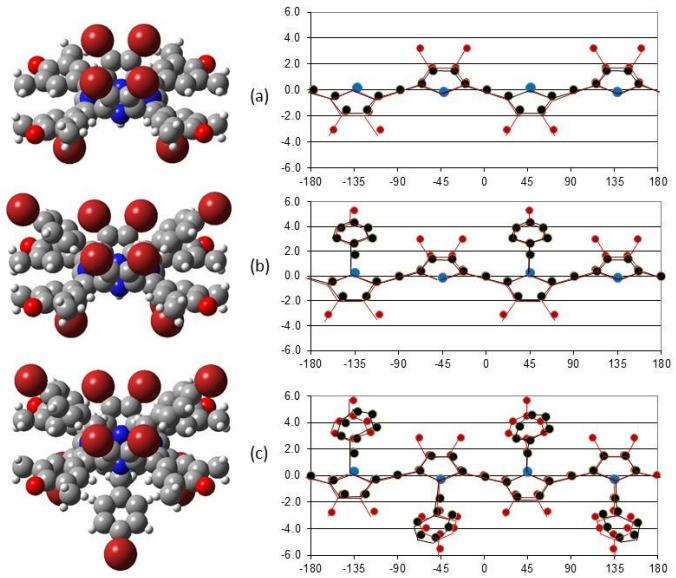

Figure 4. Space filling models of the optimized structures, and comparison of the skeletal deformations of (a) OxP and β-Br_8OxP (optimized structures) (b) the bis-N-alkylated derivatives (crystal structure) and (c) tetra N-alkylated derivatives (crystal structure). Black/blue atoms are for non-brominated compounds, red atoms denote the brominated analogues.

Compounds β-Br_8OxPBz_2 and β-Br_8OxPBz_4, bearing two and four N-benzyl substituents, respectively, exhibit macrocyclic distortions similar to compound β-Br_8OxP and their unbrominated derivatives (*ie*. the β-pyrrole carbons were displaced by ~ 1.7 Å). The position of the N-substituted benzyl groups could not exactly be matched with the X-ray structure since crystal packing makes these flexible substituents occupy less symmetric positions. Additionally, structural distortions of the computed structures of β-bromination of OxP derivatives were somewhat less important than those found in the X-ray crystal structure (< 0.1 Å), which we attribute to intermolecular crystal packing effects caused by the bulky Br substituents.

Compound	HOMO-1 (eV)	HOMO (eV)	LUMO (eV)	LUMO+1 (eV)	H-M gap (eV[a])
OxP	-5.71	-5.46	-3.46	-2.91	2.00
β-Br_8OxP	-6.12	-5.76	-3.47	-3.08	2.29
OxPBz_2	-5.70	-5.43	-3.36	-2.94	2.07
β-Br_8OxPBz_2	-6.13	-5.82	-3.48	-3.18	2.34
OxPBz_4	-5.78	-5.39	-3.28	-2.80	2.11
β-Br_8OxPBz_4	-6.26	-5.86	-3.51	-3.18	2.35

Table 3. B3LYP/3-21G calculated parameters for the investigated OxP, OxPBz_2 and OxPBz_4 and their β-pyrrole brominated derivatives.

[a]H-M = HOMO-LUMO

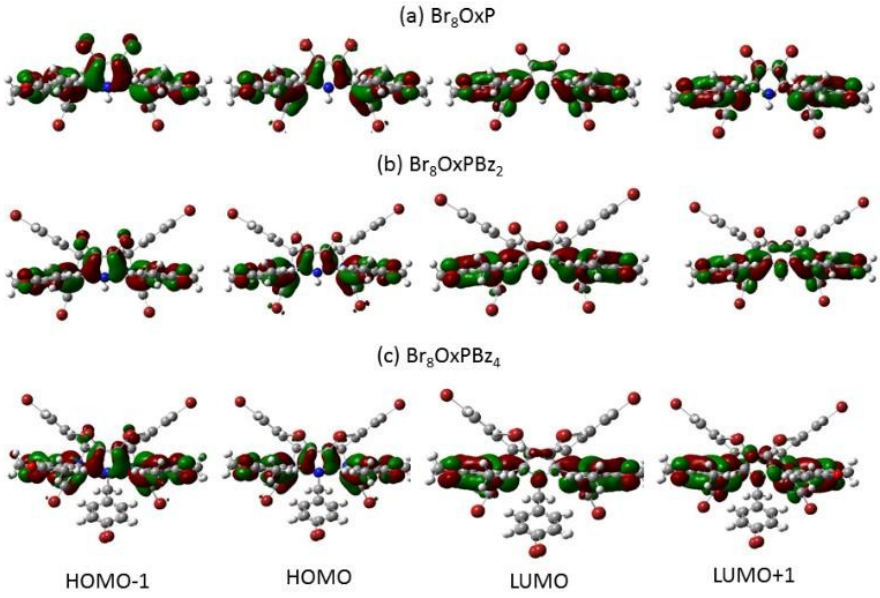

Figure 5. B3LYP/3-21G calculated frontier orbitals of brominated OxP derivatives.

Figure 5 illustrates the HOMOs and LUMOs of brominated OxP derivatives while Table 3 lists energies of these frontier orbitals along with the HOMO-LUMO gap. Similar to earlier reported frontier orbitals of OxP derivatives, the HOMOs and LUMOs of brominated OxP derivatives are all π-orbitals, spread across the oxocyclohexadienylidene rings of the porphyrinogen macrocycle due to the extension of π-conjugation of the macrocycle. The HOMOs had very little contribution while LUMOs had virtually no orbital contribution on Br substituents. The energies of both HOMOs and LUMOs were found to be perturbed upon bromination of a given OxP macrocycle (Table 3), more so for the HOMO levels. Also, the calculated HOMO-LUMO gap was found to be larger for brominated OxP compared to a given unbrominated derivative and followed the trend: β-Br_8OxP < β-Br_8OxPBz_2 < β-Br_2OxPBz_4. That is, the highest HOMO-LUMO gap was for β-Br_8OxPBz_4, a result that agreed well with the trend in absorbance spectra (blue spectral shifts upon N-alkylation of brominated OxP derivatives), discussed earlier. Additional computational studies including TD-DFT calculations on anion binding of OxP and brominated OxP is in progress and will be reported in due course.

Electrochemical and Spectroelectrochemical Studies

Since the computational studies predicted that (i) the HOMO level would be perturbed more than the LUMO level, and that (ii) the HOMO-LUMO gap increases by increasing the number of N-substituents, cyclic voltammetry studies on brominated OxP were performed and the data was compared to the earlier reported results for OxP derivatives. Figure 6 shows cyclic voltammograms of brominated OxP derivatives with redox data along with those of OxP derivatives being shown in Table 4. For the large part, the voltammograms were ill-defined with a combination of reversible, quasi-reversible and irreversible redox processes. The brominated OxP derivatives undergo reversible to irreversible oxidation and reduction processes (as judged by plots of peak current vs. square root of scan rate[37]). As predicted by computational studies, the following trends were found: (i) more difficult oxidation but easier reduction upon bromination of a given OxP derivative; (ii) greater variation in the magnitude of the oxidation potential between OxP and brominated OxP derivatives compared to that observed for the reduction potential of the respective derivative; and (iii) increases in the HOMO-LUMO gap upon

bromination for each OxP derivative in agreement with the observed blue shift in the absorbance spectrum. In summary, there is a very good agreement between the theoretical predictions and experimental results obtained for the series of OxP and brominated OxP derivatives investigated in the present study.

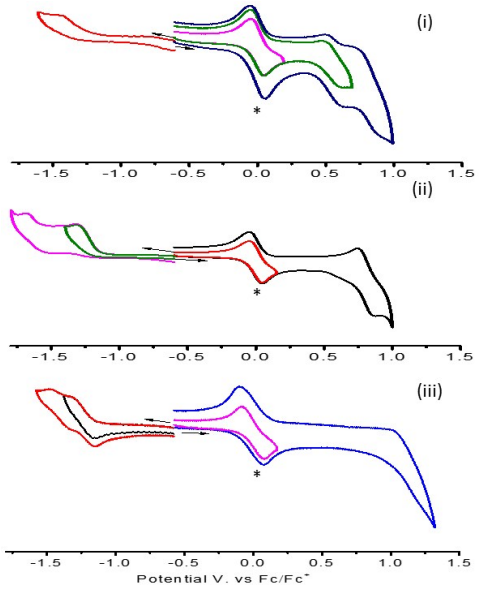

Figure 6. Cyclic voltammograms of (i) β-Br_8OxP, (ii) β-Br_8OxPBz_2 and (iii) β-Br_8OxPBz_4 in DCB containing 0.1 M (TBA)PF_6. Scan rate = 100 mV/s. The '*' represents ferrocene redox couple used as an internal standard.

Table 4: Electrochemical Redox Potentials (V Vs Fc/Fc^+) of OxP and brominated OxP derivatives in *o*-dichlorobenzene, 0.1M (TBA)PF_6

Compound	Oxidation		Reduction	
	2	1	1	2
OxP	0.48	0.27	-1.33	--
β-Br_8OxP	0.79	0.56	-1.46[a]	--
OxPBz_2	0.69	0.48	-1.38	-1.45
β-Br_8OxPBz_2	--	0.81[b]	-1.31[a]	-1.68[a]
OxPBz_4	--	0.73	-1.34	-1.38
β-Br_8OxPBz_4	--	1.20[a]	-1.22[b]	-1.40[b]

[a]-irreversible redox process, peak potential
[b]-quasi-reversible redox process

In order to spectroscopically characterize the oxidized and reduced products and pursue any trends in spectral behaviour, spectroelectrochemical studies were performed. In these measurements an additional potential of 100 mV over the half-wave potential of a given redox couple was used to ensure complete oxidation or reduction, and the spectra were recorded as a function of time. Figure 7 shows the spectral changes observed during first oxidation and first reduction of brominated OxP derivatives while the data is given in Table 2 along with those of neutral compounds. Although isosbestic points were seen in most cases, the spectral changes were found to be almost 100% reversible for both oxidation and reduction in case of β-Br_8OxPBz_4. However, for β-Br_8OxP and β-Br_8OxPBz_2, the oxidation processes were reversible while the reduction processes were about 80% reversible within the duration of the experiment. From the figure it is clear that the degree of associated spectral changes depend on the number of N-substituents. For β-Br_8OxP with no N-substituents, new strong peaks in the 610 and 760 nm range were observed upon oxidation while, for reduction, a strong peak at 660 nm was observed. In case of β-Br_8OxPBz_2, while peaks in this spectral region were observed, the intensity of these peaks, especially for oxidation, were found to be much lower indicating diminished ε values. The associated spectral changes for β-Br_8OxPBz_4 with four N-substituents were found to be minimal during oxidation, with only a lowering in intensity of the absorption maximum peak occurring with no additional new bands being observed. Interestingly, the spectrum of the reduced species had new peaks in the 700 and 810 nm range. From this study, it is clear that the one-electron oxidized and one-electron reduced species of brominated OxP derivatives reveal distinct spectral features depending upon the nature of electrochemical process (oxidation or reduction) and the number of N-substituents on the OxP. It should be noted here that the spectral trends along with reversibility observed here are much better defined than those reported earlier for unbrominated OxP derivatives.

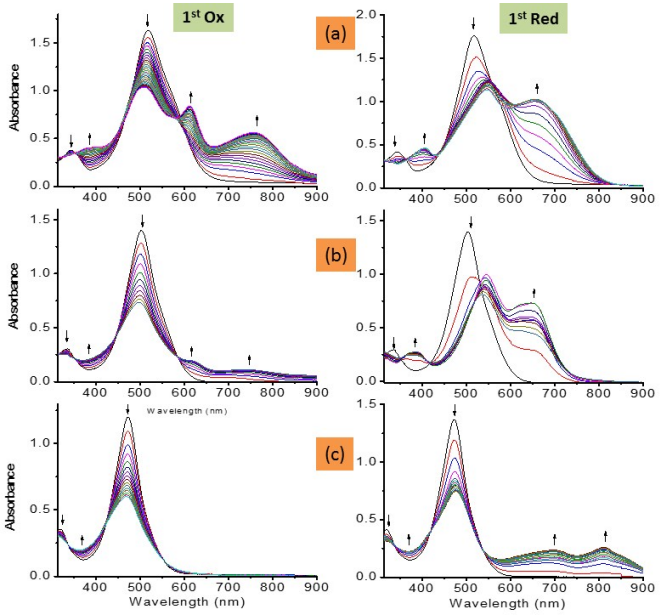

Figure 7. Spectral changes observed during first oxidation (left panel) and first reduction (right panel) of (a) β-Br_8OxP, (b) β-Br_8OxPBz_2 and (c) β-Br_8OxPBz_4 in DCB containing 0.1 M (TBA)PF_6.

Solvatochromism and Anion Binding

As shown by the X-ray structure, Br_8OxPBz_2 is found to interact with solvents, similar to that reported earlier for OxP and OxPBz_2 derivatives. However, OxPBz_4 and Br_8OxPBz_4 having no imino-hydrogens failed to reveal solvatochromic effects. Figure S2 in the supporting information show the spectra of Br_8OxP and Br_8OxPBz_2 in different solvents. Polar solvents interacted much strongly as revealed by the red-shifted absorption bands. Further, the data were analyzed utilizing solvent donor number (quantitative measurement of Lewis basicity) and the β scale of HBA (hydrogen-bond acceptor) basicities to seek linear solvation energy relationships. The β scale provides a measure

of the solvent's ability to accept a proton (donate an electron pair) in a solute-to-solvent hydrogen bond. Figure S3 illustrates the relationships between the solvent donor number, the β values, and the spectral shifts of Br_8OxP and Br_8OxPBz_2 while the data are given in Table S1. The almost linear trend in the plots suggests that solute-solvent hydrogen bonding is primarily responsible for the observed solvatochromic effect of brominated OxP. The appreciable scattering seen here could be due to different size and shape effects of the solvents.

Table 5. Spectral shifts upon anion binding and anion binding constants for Br_8OxP and Br_8OxPBz_2 derivatives in DCB.

	β-Br_8OxP		β-Br_8OxPBz_2	
Anion	Δλ, cm^{-1}	K_1, $M^{-1,a}$	Δλ, cm^{-1}	K, M^{-1}
F^-	2696	2.0 x 10^5	2135	3.5 x 10^5
Cl^-	1446	5.4 x 10^4	975	1.1 x 10^5
Br^-	841	7.3 x 10^4	856	5.3 x 10^4
I^-	866	6.5 x 10^4	764	1.6 x 10^3
PF_6^-	124	1.3 x 10^3	42	6.6 x 10^3
ClO_4^-	499	1.6 x 10^3	289	8.7 x 10^3
NO_3^-	863	2.9 x 10^4	530	4.7 x 10^3
$C_2H_3O_2^-$	1914	1.1 x 10^5	2101	5.3 x 10^5

[a]-only K_1 is reported

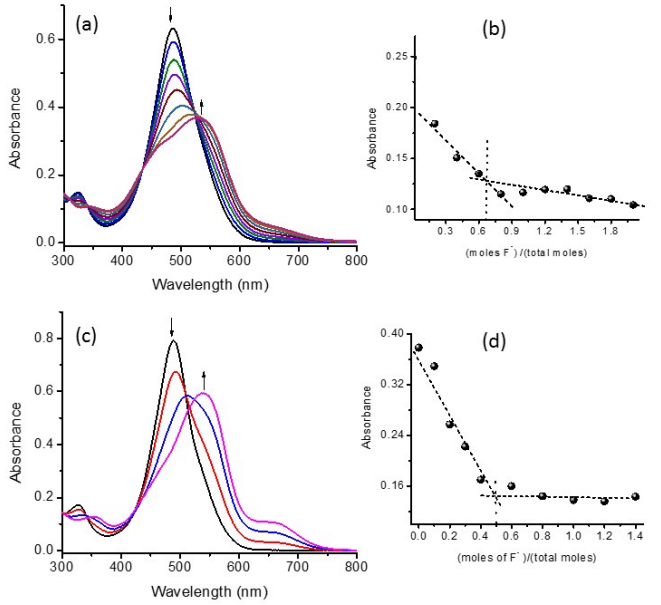

Figure 8. Spectral changes observed upon increasing addition of F^- to (a) β-Br_8OxP and (c) β-Br_8OxPBz_2 in DCB. Figures b and d show mole ratio plots constructed to evaluate anion binding stoichiometry (absorbance of 492 nm for β-Br_8OxP and of 484 nm for β-Br_8OxPBz_2 was monitored).

Further, anion binding ability of brominated OxP derivatives was investigated. In agreement with solvatochromic results, Br_8OxPBz_4 did not exhibit any appreciable anion binding ability. Figures 8a and c show the spectral changes observed during fluoride binding to Br_8OxP and Br_8OxPBz_2, respectively. New spectral features associated with one or more isosbestic points were observed. This was also the case for other employed anions (see Figure S4 for representative plots). In order to evaluate the stoichiometry, plots of continuous variation were constructed. In agreement with binding stoichiometries of OxP and OxPBz_2, a 2:1 stoichiometry for F^- binding to Br_8OxP and 1:1 stoichiometry for F^- binding to Br_8OxPBz_2 (see Figures 8b and d) were established. The binding constants were also evaluated by constructing Benesi-Hildebrand plots. These data along with spectral shifts are given in Table 5 for the anions studied. The magnitudes of binding constants were generally higher than those reported earlier for OxP and OxPBz_2 derivatives, a result that can be easily rationalized according to the increased Lewis acidity of brominated OxP derivatives having electron withdrawing halogen substituents. As expected, higher binding constants for most basic anions (conjugate bases of weak acids) was observed.

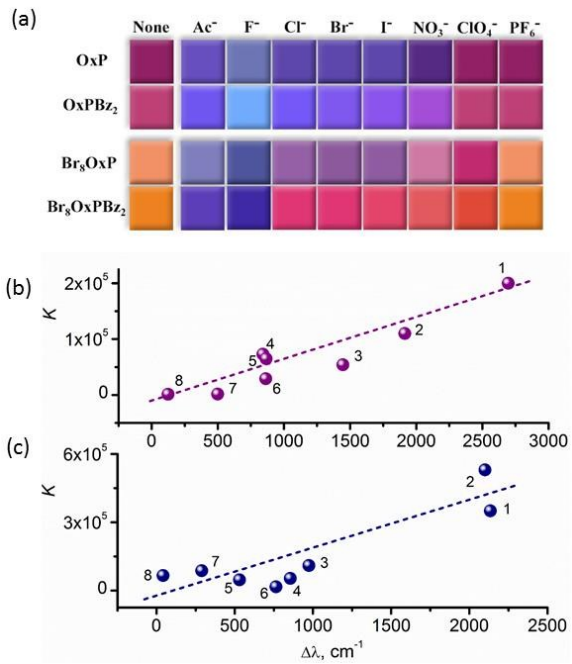

Figure 9. (a) Tiling representation of the colours of dilute (~5 X 10^{-6} mol in DCB) solutions of OxP, OxPBz_2, β-Br_8OxP and β-Br_8OxPBz_2 in the presence of various anions. Plots of binding constant of different anions versus spectral shift for (b) β-Br_8OxP and (c) β-Br_8OxPBz_2. 1: F^-, 2:acetate, 3:Cl^-, 4:Br^-, 5:I^-, 6:NO_3^-, 7:ClO_4^- and 8:PF_6^-.

The spectral shifts of the absorbance peak were correlated with the K values as shown in Figure 9b and c. Linear trends were observed for both of the investigated brominated porphyrinogen derivatives. We have previously reported similar trends for OxP and OxPBz_2 derivatives. Together with the results of solvatochromic studies shown in Figure S2, these results conclusively indicate that hydrogen bonding interactions are primarily responsible for these observations. As mentioned earlier, it should be noted that deviation of data points from linearity could be due to the effects of dimensions and morphology of the solvent molecules. In an effort to seek anion binding selectivity in a qualitative fashion, the colorimetric responses of oxoporphyrinogens to various anions were investigated. As shown in Figure 9a, all four OxP compounds give visible responses to anions depending upon their anion binding strength. For example, strongly binding anions such as fluoride and acetate lead to blue or blue-violet colours

compared to the initial pink-red of OxP derivatives and dark yellow-orange of the brominated OxP derivatives. Weakly binding anion such as PF_6^- do not cause a change in colour although presence of perchlorate anions leads to a change in hue for brominated OxPs but not the non-brominated analogues. This suggests that further tuning of the OxP structure by introduction of functionality can be used as a means to tune the properties of OxP compounds; this is a feature we continue to investigate. For anions of intermediate binding strengths, colour is dependent on the nature of the OxP receptor. For example, for NO_3^- binding, dark blue for OxP, violet for $OxPBz_2$, brown-pink for β-Br_8OxP and dark orange for β-Br_8OxPBz_2 were observed. Therefore, we expect that a class of OxP derivatives containing a similar receptor but with differing chemical structures and optical responses to anions can be used in the design of 'optoelectronic noses' operating based on colorimetric sensor arrays. Such studies are in progress in our laboratories.

Conclusions

A relatively simple procedure involving direct bromination of 5,10,15,20-tetrakis(3,5-di-t-butyl-4-hydroxyphenyl)porphyrinatocopper(II) to yield β-pyrrole brominated oxoporphyrinogen has been developed. During bromination, both oxidation and demetallation of the porphyrin derivative occurred to yield the required brominated OxP product. Further, N-alkylation reaction was performed to produce bis-N-alkylated and tetra-N-alkylated brominated OxP products. The X-ray structure of N-alkylated derivatives and computational results revealed saddle shaped distortion of the OxP macrocycle irrespective of the N-substituents. Interestingly, although both OxP and brominated OxP macrocycles were severely distorted, the degree of ring distortion for brominated OxP derivatives was only slightly greater than that of unbrominated OxP derivatives although according to crystallographic data opposing pyrrole rings subtend much more acute angles in the brominated derivatives. Absorbance, electrochemical and spectroelectro- chemical studies yielded results in support of theoretical predictions of (i) HOMO levels vary to a greater extent (become increasingly negative relative to the non-brominated analogues) than the LUMO level upon bromination, and (ii) increased HOMO-LUMO gap revealing blue-shift absorbance bands upon increasing the N-substituents. Both β-Br_8OxP and β-Br_8OxPBz_2 having 4 or 2 imino-hydrogens, respectively, and not β-Br_8OxPBz_4 lacking imino-hydrogens, revealed solvotochromic and anion binding effects. A 1:2 and 1:1 stoichiometry was established, respectively, for β-Br_8OxP and β-Br_8OxPBz_2 binding to anions. The measured binding constants were found to be higher compared to those reported earlier for the corresponding OxP derivatives due to induced effects caused by the electron withdrawing bromo substituents. The colorimetric sensor studies suggest that the OxP compounds reported here are likely candidates for designing optoelectronic noses for detecting anions and other anionic species of biological interest.

Acknowledgements

The authors are grateful to the National Science Foundation (Grant No. 1401188 to FD) and to the World Premier International Research Centre Initiative (WPI Initiative) on Materials Nanoarchitectonics, from Ministry of Education, Culture, Sports, Science and Technology (MEXT), Japan for support of this work. The computational work was performed at the Holland Computing Centre of the University of Nebraska.

Notes and references

‡ Crystallographic data (excluding structure factors) have been deposited with the Cambridge Crystallographic Data Centre with CCDC reference number 1432659 (for β-Br_8OxPBz_2). Copies of the data can be obtained, free of charge, on application to CCDC, 12 Union Road, Cambridge CB2 1EZ, UK http://www.ccdc.cam.ac.uk/perl/catreq/catreq.cgi, e-mail: data_request@ ccdc.cam.ac.uk, or fax: +44 1223 336033.

1 (a) P. A. Gale and T. Gunnlaugsson, (Eds) Special themed issue on Supramolecular Chemistry of Anionic Species, *Chem. Soc, Rev.*, 2010, **39**, issue 10; (b) P. A. Gale, *Coord. Chem. Rev.*, 2000, **199**, 181; (c) *Supramolecular Chemistry of Anions*; Bianchi, A.; Bowman-James, K.; Garcia-Espana, E., Eds.; VCH: Weinheim, 1997.

2 (a) A.-F. Li, J.-H. Wang, F. Wang and Y.-B. Jiang, *Chem. Soc. Rev.*, 2010, **39**, 3729; (b) V. Amendola, L. Fabbrizzi and L. Mosca, *Chem. Soc. Rev.*, 2010, **39**, 3889.

3 (a) S. E. Matthews and P. D. Beer, *Supramol. Chem.*, 2005, **17**, 411; (b) A. Casnati, F. Sansone and R. Ungaro, *Adv. Supramol. Chem.*, 2003, **9**, 163; (c) B. Mokhtari and K. Pourabdollah, *Asian J. Chem.*, 2011, **23**, 4717.

4 (a) K. Choi and A. D. Hamilton, *Coord. Chem. Rev.*, 2003, **240**, 101; (b) K. Bowman-James, *Acc. Chem. Res*., 2005, **38**, 671; (c) S. O. Kang, J. M. Llinares, V. W. Day and K. Bowman-James, *Chem. Soc. Rev*., 2010, **39**, 3980.

5 A. Nori de Macedo, M. I. Y. Jiwa, J. Macri, V. Belostotsky, S. Hill and P. Britz-McKibbin, *Anal. Chem.,* 2013, **85**, 11112 and references cited therein.

6 J. R. Erichsen Jones, *J. Exp. Biol.*, 1941, **18**, 170.

7 (a) J. Wu, B. Kwon, W. Liu, E. V. Anslyn, P. Wang and J. S. Kim, *Chem. Rev.*, 2015, **115**, 7893; (b) A. Vargas-Jentzsch, A. Hennig, J. Mareda and S. Matile, *Acc. Chem. Res.*, 2013, **46**, 2791; (c) N. A. Esipenko, P. Koutnik, T. Minami, L. Mosca, V. M. Lynch, G. V. Zyryanov and P. Anzenbacher, *Chem. Sci.*, 2013, **4**, 3617; (d) R. Nishiyabu and P. Anzenbacher, *Org. Lett.*, 2006, **8**, 359; (e) Z. Zhang, D. S. Kim, C.-Y. Lin, H. Zhang, A. D. Lammer, V. M. Lynch, I. Popov, O. S. Miljanic, E. V. Anslyn and J. L. Sessler, *J. Am. Chem. Soc.*, 2015, **137**, 7769; (f) A. P. de Silva, D. B. Fox, A. J. M. Huxley, N. D. McClenaghan and J. Roiron, *Coord. Chem. Rev.*, 1999, **185-186**, 297; (g) M. J. Langton and P. D. Beer, *Chem. Eur. J.*, 2012, **18**, 14406; (h) A. Caballero, F. Zapata, and P. D. Beer, *Coord. Chem. Rev.*, 2013, **257**, 2434.

8 P. A. Gale, R. Pérez-Tomás and R. Quesada, *Acc. Chem. Res*., 2013, *46*, 2801.

9 (a) N. R. Williamson, P. C. Fineran, T. Gristwood, S. R. Chawrai, F. J. Leeper and G. P. C. Salmond, *Future Microbiol*., 2007, **2**, 605; (b) R. Perez-Tomas, B. Montaner, E. Llagostera and V. Soto-Cerrato, *Biochem Pharm*., 2003, **66**, 1447; (c) K. Papireddy, M. Smilkstein, J. X. Kelly, Shweta, S. M. Salem, M. Alhamadsheh, S. W. Haynes, G. L. Challis and K. A. Reynolds, *J. Med. Chem*., 2011, **54**, 5296; (d) J.-C. Su, K.-F. Chen, W.-L. Chen, C.-Y. Liu, J.-W. Huang, W.-T. Tai, P.-J. Chen, I. Kim and C.-W. Shiau, *Eur. J. Med. Chem*., 2012, **56**, 127; (e) D. A.

Smithen, A. M. Forrester, D. P. Corkery, G. Dellaire, J. Colpitts, S. A. McFarland, J. N. Berman and A. Thompson, *Org. Biomol. Chem.*, 2013, **11**, 62.
10 (a) J. L. Sessler, P. A. Gale and J. W. Genge, *Chem. Eur. J.*, 1998, **4**, 1095; (b) P. A. Gale and C.-H. Lee, *Top. Heterocycl. Chem.*, 2010, **24**, 39; (c) A. Aydogan, D. J. Coady, V. M. Lynch, A. Akar, M. Marquez, C. W. Bielawski and J. L. Sessler, *Chem. Commun.*, 2008, **12**, 1455; (d) R. Custelcean and B. A. Moyer, *Eur. J. Inorg. Chem.*, 2007, 1321; (e) J. Wang, R. G. Harrison and J. D. Lamb, *J. Chromatogr. Sci.*, 2009, **47**, 510; (f) A. El-Hashani, A. Toutianoush and B. Tieke, *J. Phys. Chem. B* 2007, **111**, 8582; (g) X. Zhao, X. Bu, T. Wu, S.-T. Zheng, L. Wang and P. Feng, *Nat. Commun.*, 2013, **4**, ncomm2344; (h) S. Fukuzumi, K. Ohkubo, F. D'Souza and J. L. Sessler, *Chem. Commun*., 2012, **48**, 9801.
11 (a) D. S. Kim and J. L. Sessler, *Chem. Soc. Rev.*, 2015, **44**, 532; (b) S. Camiolo, P. A. Gale and J. L. Sessler, in *Encyclopedia of Supramolecular Chemistry*, Atwood, J. L.; Steed, J. W., Eds. Marcel Dekker: New York, 2004; (c) P. A. Gale, J. L. Sessler and V. Král, *Chem. Commun*., 1998, 1.
12 P. A. Gale, J. L. Sessler, V. Král and V. Lynch, *J. Am. Chem. Soc.*, 1996, **118**, 5140.
13 J. L. Sessler, S. K. Kim, D. E. Gross, C.-H. Lee, J. S. Kim and V. M. Lynch, *J. Am. Chem. Soc.*, 2008, **130**, 13162.
14 P. A. Gale, J. L. Sessler, W. E. Allen, N. A. Tvermoes amd V. M. Lynch, *Chem. Commun.*, 1997, 665.
15 S. Dey, K. Pal and S. Sarkar, *Tetrahedron Lett*., 2008, **49**, 960.
16 D. E. Chumakov, A. V. Khoroshutin, A. V. Anisimov and K. I. Kobrakov, *Chem. Heterocycl. Compd.*, 2009, **45**, 259.
17 (a) J. P. Hill, A. L. Schumacher, F. D'Souza, J. Labuta, C. Redshaw, M. R. J. Elsegood, M. Aoyagi, T. Nakanishi and K. Ariga, *Inorg. Chem.*, 2006, **45**, 8288; (b) A. L. Schumacher, J. P. Hill, K. Ariga and F. D'Souza, *Electrochem, Commun*., 2007, **9**, 2751.
18 (a) L. R. Milgrom, *Tetrahedron*, 1983, **39**, 3895; (b) J. P. Hill, F. D'Souza and K. Ariga, in *Supramolecular Chemistry: From Molecules to Nanomaterials*, Gale, P. A.; Steed, J. W. (Eds.) 2012 John Wiley & Sons, pp 1713.
19 (a) J. P. Hill, I. J. Hewitt, C. E. Anson, A. K. Powell, A. L. McCarty, P. A. Karr, M. E. Zandler and F. D'Souza, *J. Org. Chem*., 2004, **69**, 5861; (b) E. Dolušić, S. Toppet, S. Smeets, L. V. Meervelt, B. Tinant and W. Dehaen, *Tetrahedron*, 2003, **59**, 395; (c) J. P. Hill, W. Schmitt, A. L. McCarty, K. Ariga and F. D'Souza, *Eur. J. Org. Chem*., 2005, 2893.
20 F. D'Souza, N. K. Subbaiyan, Y. Xie, J. P. Hill, K. Ariga, K. Ohkubo and S. Fukuzumi, *J. Am. Chem. Soc.*, 2009, **131**, 16138.
21 J. Labuta, Z. Futera, S. Ishihara, H. Kourilova, Y. Tateyama, K. Ariga and J. P. Hill, *J. Am. Chem. Soc.*, 2014, **136**, 2112.
22 M. Valiev, E. J. Bylaska, N. Govind, K. Kowalski, T. P. Straatsma, H. J. J. van Dam, D. Wang, J. Nieplocha, E. Apra, E. L. Windus and W. A. de Jong, *Comput. Phys. Commun*., 2010, **181**, 1477.
23 P. Byhrappa and V. Krishnan, *Inorg. Chem.*, 1991, **30**, 239.
24 P. J. Commins, J. P. Hill, Y. Matsushita, W. A. Webre, F. D'Souza, K. Ariga, *J. Porphyrins Phthalocyanines*, 2015, in press.
25 *CrystalClear,* Rigaku Corporation, Tokyo, Japan (2005).
26 G. M. Sheldrick, *Acta Cryst.*, 2015, **A71**, 3.
27 G. M. Sheldrick, *Acta Cryst.*, 2008, ***A*64**, 112.
28 L. J. Farrugia, *J. Appl. Cryst.*, 1999, **32**, 837.
29 R. A. Richards, K. Hammons, M. Joe and G. M. Miskelly, *Inorg. Chem.*, 1996, **35**, 1940.
30 (a) H. J. Callot, *Bull. Soc. Chim. Fr.*, 1974, 1492; (b) T. G. Traylor and S. Tsuchiya, *Inorg. Chem.*, 1987, **26**, 1338.
31 (a) L. R. Milgrom, N. Mofidi, C. C. Jones and A. Harriman, *J. Chem. Soc., Perkin Trans. 2*, 1989, 301; (b) L. R. Milgrom, N. Mofidi and A. Harriman, *J. Chem. Soc., Perkin Trans. 2*, 1989, 805; (c) L. R. Milgrom, N. Mofidi and A. Harriman, *Tetrahedron*, 1989, **45**, 7341; (d) L. R. Milgrom, W. D. Flitter and E. L. Short, *J. Chem. Soc., Chem. Comm.*, 1991, 788; (e) L. R. Milgrom, J. P. Hill and W. D. Flitter, *J. Chem. Soc., Chem. Comm.*, 1992, 773.
32 L. R. Milgrom and J. P. Hill, *J. Heterocycl. Chem.*, 1993, **30**, 1629.
33 A. J. Golder, L. R. Milgrom, K. B. Nolan and D. C. Povey, *Acta Cryst.*, 1988, **C44**, 1916.
34 A. J. Golder, L. R. Milgrom, K. B. Nolan and D. C. Povey, *J. Chem. Soc., Chem. Comm*., 1989, 1751.
35 (a) J. Labuta, S. Ishihara, T. Šikorský, Z. Futera, A. Shundo, L. Hanyková, J. V. Burda, K. Ariga, J. P. Hill, *Nat. Commun.*, 2013, **4**, ncomm2188. (b) J. Labuta, S. Ishihara, K. Ariga and J. P. Hill, *Symmetry*, 2014, **6**, 345.
36 R. Gutzler, C. Fu, A. Dadvand, Y. Hua, J. M. MacLeod, F. Rosei and D. F. Perepichka, *Nanoscale*, 2012, **4**, 5965.
37 J. Heinze, *Angew. Chem. Int. Ed.,* 1984, **23**, 831.

Table of content

Anion Binding, Electrochemistry and Solvatochromism of β-Brominated Oxoporphyrinogens

W. A. Webre, J. P. Hill,* Y. Matsushita, P. A. Karr, K. Ariga and F. D'Souza*

A series of β-pyrrole brominated oxoporphyrinogens have been synthesized, and their physicochemical properties relevant to structure-activity are investigated.

Table of Contents